

Dynamic Modelling and Analysis of Safety Aspects of Vehicle Side Impact

Yaojun Zheng, Yong Feng, Kaikao Chen

Zhejiang Technical Institute of Economics, HangZhou, Zhejiang, 310018

Abstract — Studies on the safety of vehicle side impact has become an important research area in the field of automotive passive safety. In this paper we establish the nonlinear dynamic model and its simulation as explicit computations using finite element methods. We use the finite element model of vehicle side stiffness to carry out impact simulation analysis. Our simulation and result analysis will be helpful to improve the safety performance of side impact in vehicles.

Keywords — *vehicle side crash safety; dynamics modelling; finite element methods*

I. INTRODUCTION

With the rapid development of economy in china, the car is playing an increasingly important role in people's daily life. However, with the rapid increase of car ownership, it also leads to a variety of traffic accidents, not only caused a huge loss of property, but also serious threat to people's lives and safety. In all kinds of traffic accidents, frontal crash and side impact are the highest frequency and side impact, which is the accident form and the highest casualty rate. Therefore, vehicle side impact safety research has become an important research content in the field of automotive passive safety [1].

Acar E proposed the reliability design of the system based on the vehicle impact resistance and all kinds of uncertainties [2]. Fang H proposed Numerical simulations of multiple vehicle collision accident and multidisciplinary crashworthiness optimization method [3]. Improving accuracy of vehicle crashworthiness response predictions using ensemble of metamodels was also given by Acar E [4]. Automated vehicle structural crashworthiness design via a crash mode matching algorithm was proposed by Hamza K [5]. A two-stage multi-objective optimization method of vehicle crashworthiness under frontal impact was proposed by Liao XT[6]. Crashworthiness design optimization method of metal honeycomb energy absorber used in lunar lander was proposed by LI Meng[7]. Multiobjective optimization method of multi-cell sections for the crashworthiness design was proposed by HOU Shu-juan[8]. Optimizing crashworthiness design of square honeycomb structure was proposed by Meng Li[9]. A Comparative study on multi-objective reliable and robust optimization for crashworthiness design of vehicle structure was given by Xianguang Gu[10], that takes a typical vehicle structure subject to offset frontal crashing scenario as an example to compare reliable and robust designs with their deterministic counterpart. Multi-objective robust optimization method for crashworthiness during side impact was proposed by Sinha K[11]. Crashworthiness design of vehicle by using multi-objective robust optimization was proposed

by Sun GY[12]. Crushing analysis and multi-objective crashworthiness optimization of honeycomb-filled single and bitubular polygonal tubes was given by Yin HF[13]. Crashworthiness design of vehicle by using multi-objective robust optimization. Structural and Multidisciplinary Optimization was proposed by Guangyong Sun[14]. Automotive crashworthiness design using response surface-based variable screening and optimization was proposed by Craig KJ[15]. A method for selecting surrogate models in crashworthiness optimization was proposed by Lei Shi[16]. Probability-based least square support vector regression meta modelling technique for crashworthiness optimization problems was proposed by Hu Wang [17]. Multipoint version of space mapping optimization applied to vehicle crashworthiness design was proposed by Redhe M [18].

In the next section, the nonlinear dynamic explicit finite element method is investigated. In Section 3, side crash finite element model validation is given. In section 4, the simulation calculation and result analysis of side crash is given. Finally, some conclusions are given in section 5.

II. THE NONLINEAR DYNAMIC EXPLICIT FINITE ELEMENT METHOD

Vehicle crash is a very complex dynamics problem, in the process of vehicle crash, the crash process has highly nonlinear property, such as geometric nonlinearity, material nonlinearity and contact nonlinearity etc., so choosing a suitable calculation theory for vehicle crash simulation analysis is particularly important. In the vehicle crash simulation analysis, the numerical simulation methods are mainly multi-rigid-body dynamics research method and nonlinear dynamic display finite element method. The former mainly studies the response of human body and vehicle parts. This paper mainly studies vehicle side crashworthiness and the nonlinear dynamic display finite element method is used for vehicle crash simulation and analysis.

At initial time, the coordinates of the particle is $X_i(i=1,2,3)$. The coordinates of the particle at any time t is $x_i(i=1,2,3)$, the movement equation of the particle is $x_i = x_i(X_j, t)$. The initial condition at time 0 is $x_i(X_j, 0) = X_j$, $\dot{x}_i(X_j, 0) = V_i(X_j, 0)$.

V_i represents the initial speed. The momentum conservation equation is $\delta_{ij,j} + \rho f_i = \rho \ddot{x}_i$.

$$\delta_{ij} \text{ represents Cauchy stress, } \delta_{ij,j} = \frac{\partial \delta_{ij}}{\partial x_j}, f_i$$

represents unit mass volume force, \ddot{x}_i represents acceleration and ρ represents mass density. The mass conservation equation is

$$\rho = J \rho_0$$

ρ_0 represents mass density at initial time and J represents change coefficient of system density. Energy

$$\text{conservation equation is } E = V \delta_{ij} \varepsilon_{ij} - (p + q)V$$

This equation is used for calculation of state equation and the overall energy balance. V represents

the volume of the current configuration, ε_{ij} represents strain rate tensor, P represents pressure and q represents volume viscous resistance. The boundary

$$\text{condition of surface force } s^1 \text{ is } \delta_{ij} n_j = T_i(t)$$

$n_j(j=1,2,3)$ represents direction cosine of the outward normal, $T_i(i=1,2,3)$ represents the surface

force load. The boundary condition of s^2 displacement is $X_i(X_j, t) = K_i(t)$.

$K_i(t)$, $i=1,2,3$ represents the known displacement linear function. Specific algorithm of the explicit integral algorithm is as follows.

The dynamics equilibrium equation is

$$u_{(t)} = M^{-1} \cdot (P_{(t)} - I_{(t)})$$

The explicit integral of time is

$$u_{(t+\frac{\Delta t}{2})} = u_{(t-\frac{\Delta t}{2})} + \frac{(\Delta t_{(t+\Delta t)} + \Delta t_{(t)})}{2} u_{(t)}$$

$$u_{(t+\Delta t)} = u_{(t)} + \Delta t_{(t+\Delta t)} u_{(t+\frac{\Delta t}{2})}$$

According to the strain rate ε , calculate cell strain increment $d\varepsilon$. According to the constitutive relation, calculate stress σ , $\sigma_{(t+\Delta t)} = f(\sigma_{(t)}, d\varepsilon)$. Integrated node internal force is $I_{(t+\Delta t)}$.

The explicit central difference method is stable, only when the time step is less than the critical time step

$$\Delta t \leq \Delta t_{crit} = \frac{2}{w_{max}}$$

w_{max} represents the maximum angular frequency.

Because the natural frequency of bar, $w_{max} = 2 \frac{c}{l}$. Critical time step of the bar is

$$\Delta t = \frac{l}{c}, l \text{ and } c \text{ is determined by unit type. For}$$

quadrilateral shell element, $l = \frac{A}{\max(L_1, L_2, L_3, L_4)}$.

For triangular shell element, $l = \frac{2A}{\max(L_1, L_2, L_3)}$,

$$c = \sqrt{\frac{E}{\rho(1-\nu^2)}}$$

Due to the material properties are constant, the time step is completely determined by unit minimum size. The smaller the cell size, the smaller the time step is and the more computing resources and cost required. When the finite element model is established, it is important to note that the minimum cell size.

III. SIDE CRASH FINITE ELEMENT MODEL VALIDATION

The side crash simulation model is established according to GB 20071-2006 regulations. Mobile deformation wall vertically crashes the side of the static vehicle at a speed of 50 km/h, its Perpendicular bisector crashes side front seat through vehicle, and simulation time is 140 ms. The system overall energy change is shown in figure 1. The top green line represents total energy, the middle green line represents kinetic energy of the system, the middle red line represents internal energy, the bottom red line represents interface energy and the blue line represents hourglass energy. The horizon axis represents time, the unit of which is millisecond and the vertical axis represents energy. The sliding interface energy and the hourglass energy can keep small positive value, which is no more than 5% of the total energy. Figure 2 is the acceleration-time curve of the bottom B-pillar of the bumped side. The blue line represents simulation and the red line represents experiment. The figure shows change trend of the acceleration curve is almost the same, and peak value and turning up time is in good agreement. The existence

of the error may be because of the vehicle omitted vehicle accessories, material parameters and soldered dots, but the overall error is less than 5%. The finite element model is consistent with vehicle side stiffness, which can be used in the side crash simulation analysis.

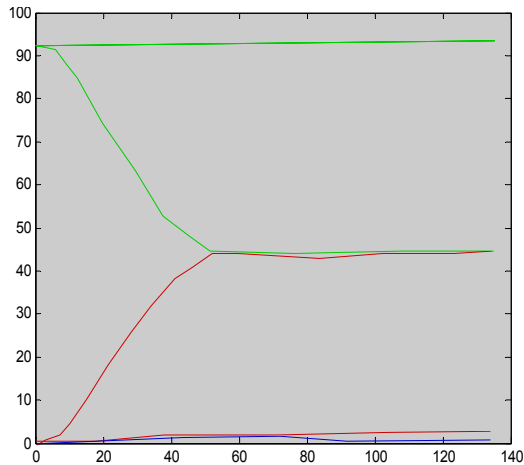


fig.1 overall energy curve

IV. SIMULATION AND ANALYSIS OF SIDE CRASH

A particular vehicle model is taken as researched object. Inside of the door plank of the left front door can damage

fake people. The research results show that the relation between chest damage value and intrusion velocity is

$$TTI = 60.60 - 0.03M + 0.93V_d - 0.12a_d + 0.70C_d$$

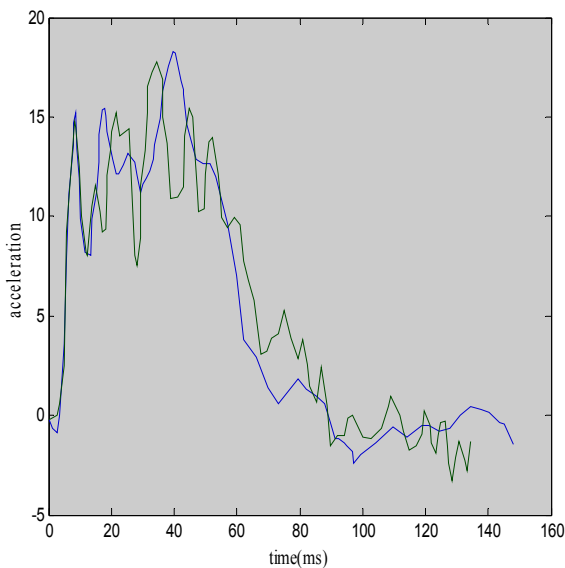


fig.2 The acceleration-time curve of the bottom B-pillar of the bumped side

Relation between damage value at pelvis location and intrusion quantity is

$$a_p = -19.1 - 0.05m + 2.02C_d + 0.04L - 0.10a_d$$

TTI represents chest injury index, *m* represents vehicle quality, V_d represents maximum intrusion speed *V* for the door. a_p represents pelvis acceleration,

C_d represents maximum intrusion quantity of door, *L* represents wheelbase and a_d represents maximum acceleration of door of vehicle. The maximum intrusion quantity and maximum intrusion speed can damage people greatly. Intrusion quantity and intrusion speed of three positions is shown in table 1. P represents collision contact area between breasts and door inside plate, Q represents collision contact area between pelvis and door inside plate. R represents B-pillar deformation biggest position area.

Reducing the intrusion capacity and speed index of the three positions can improve the body energy absorbing structure to improve side impact safety performance. If intrusion quantity and intrusion velocity is small, the side impact safety is higher.

TABLE I . INTRUSION QUANTITY AND INTRUSION SPEED OF THREE POSITIONS

position	Intrusion quantity(mm)	Intrusion speed(mm/ms)
P	330	15.5
Q	300	14.5
R	340	13.8

The intrusion quantity and speed of this vehicle is large, which cause serious damage to people's life and safety. Connection parts between B-pillar and the roof left side longitudinal beam and the threshold step has serious deformation. Stiffness of central parts of B-pillar is too weak, which cause the intrusion quantity and speed of P, Q and R is larger. Velocity curve of the B-pillar is shown in figure 3, acceleration curve of the B-pillar is shown in figure 4, door velocity curve is shown in figure 5 and door acceleration curve is shown in figure 6.

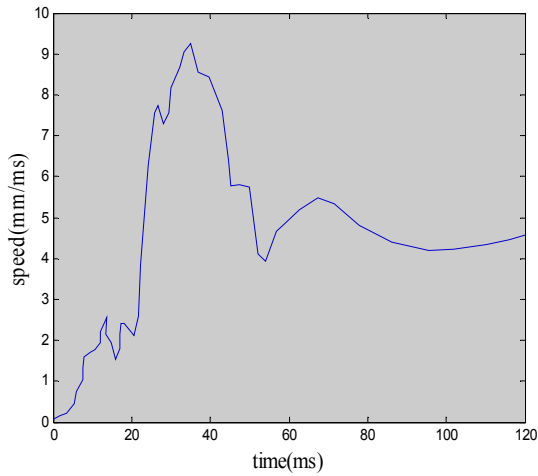


fig.3 Velocity curve of the B-pillar

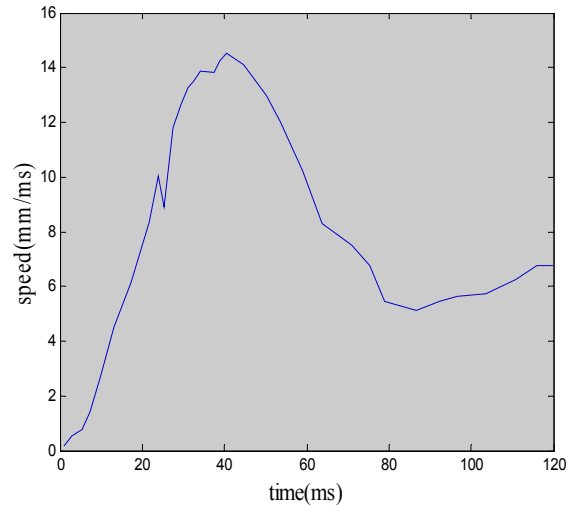


fig.5 door velocity curve

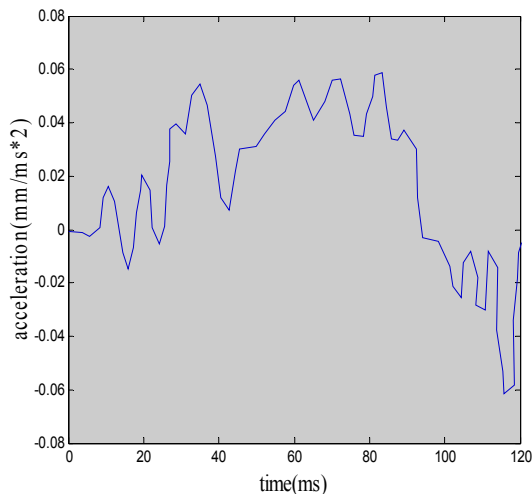


fig.4 Acceleration curve of the B-pillar

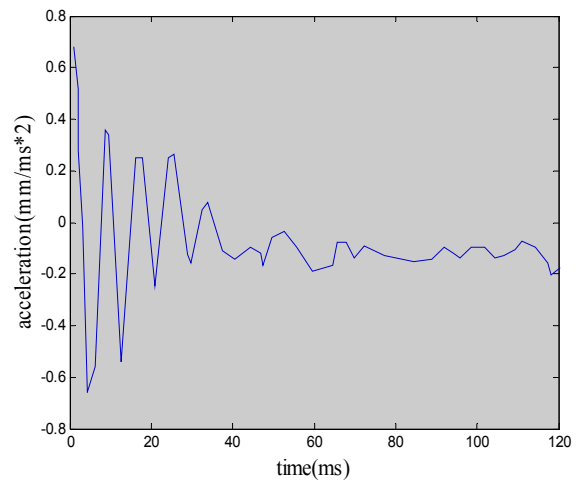


fig.6 Door acceleration curve

After the crash of 20ms, B-pillar crash speed changes gently. After the crash of 32 ms, the speed achieves the peak value 9.6 m/s. After 70ms, it gradually achieves a more stable speed. From figure 5, it can be seen that at about 40 ms, the speed achieves the peak value 14.7 m/s, which takes place within a few milliseconds after crash has just started. There is only 20 to 30 centimetres between people and the door, so that the crash impact is bigger.

V. CONCLUSIONS

At last, some principles are given to improve side crashworthiness of vehicle. B-pillar buckling deformation and excessive varus deformation should not occur. Deformation velocity curve of the lower part of the front and rear door is shown in figure 7 after optimization and invasive of response curve of the lower part of the front and rear door after optimization is shown in figure 8.

The anti-collision board inside the door has enough stiffness and it does not produce too much bending deformation. Top beam and stringer connected with B-pillar must have enough stiffness and buckling deformation and excessive varus deformation should not occur. Floor beam should have enough stiffness and force transmission capability. The door threshold has larger contact area with the lower edge to reduce the intrusion of the door. The maximum deformation position of B-pillar is at the bottom as far as possible.

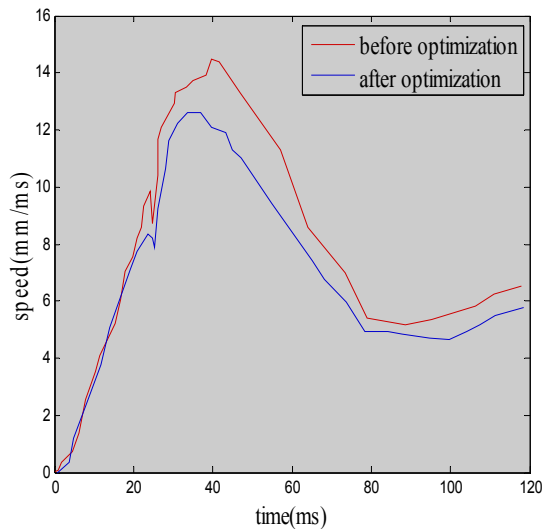


fig.7 Deformation velocity curve of the lower part of the front and rear door

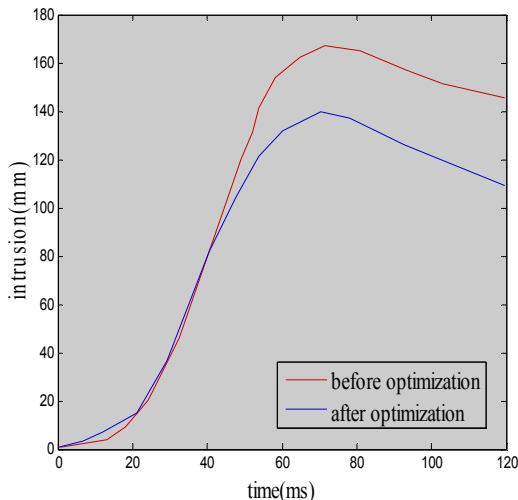


fig.8 Invasive of response curve of the lower part of the front and rear door

ACKNOWLEDGMENT

This work is supported by the Science and Technology Department of Zhejiang Province in 2013 project “Internet based specialty car simulation training platform to build” (NO. 2013C31077)

REFERENCES

[1] Kurtaran H, Eskandarian A, Marzougui D, Bedewi NE, “Crashworthiness design optimization using successive response surface approximations”, *Comput Mech*, 29(4-5), 409-421, 2002.

[2] Acar E, Solanki KN, “System reliability based vehicle design for crashworthiness and effects of various uncertainty reduction measures”, *Struct Multidiscip Optim*, 39(3), 311-325, 2009.

[3] Fang H, Solanki KN, Horstemeyer MF, “Numerical simulations of multiple vehicle crashes and multidisciplinary crashworthiness optimization”, *International Journal of Crashworthiness*, 10(2), 161-171, 2004.

[4] Acar E, Solanki KN, “Improving accuracy of vehicle crashworthiness response predictions using ensemble of metamodels”, *International Journal of Crashworthiness*, 14(1), 49-61, 2009.

[5] Hamza K, Saitou, K, “Automated vehicle structural crashworthiness design via a crash mode matching algorithm. Transactions of ASME”, *Journal of Mechanical Design*, 133(1), 011003-1-011003-9, 2011.

[6] Liao XT, Li Q, Yang XJ, Li W, Zhang WG, “A two-stage multi-objective optimisation of vehicle crashworthiness under frontal impact”, *International Journal of Crashworthiness*, 13(3), 279-288, 2008.

[7] LI Meng, DENG Zong-quan, LIU Rong-qiang, GUO Hong-wei, “Crashworthiness design optimisation of metal honeycomb energy absorber used in lunar lander”, *International Journal of Crashworthiness*, 16(4), 411-419, 2011.

[8] HOU Shu-juan, LI Qing, Long Shu-yao, YANG Xu-jing, LI Wei, “Multiobjective optimization of multi-cell sections for the crashworthiness design”, *International Journal of Impact Engineering*, 35(11), 1355-1367, 2008.

[9] Meng Li, Zong-quan Deng, Hong-wei Guo, Rong-qiang Liu, Beichen Ding, “Optimizing crashworthiness design of square honeycomb structure”, *Journal of Central South University*, 21(3), 912-919, 2014.

[10] Xiangguang Gu, Guangyong Sun, Guangyao Li, Lichen Mao, Qing Li, “A Comparative study on multiobjective reliable and robust optimization for crashworthiness design of vehicle structure”, *Structural and Multidisciplinary Optimization*, 48(3), 669-684, 2013.

[11] Sinha K, Krishnan R, Raghavendra D, “Multiobjective robust optimisation for crashworthiness during side impact”, *Int J Veh Des*, 43(1-4), 116-135, 2007.

[12] Sun GY, Li GY, Zhou SW, Li HZ, Hou SJ, Li Q, “Crashworthiness design of vehicle by using multiobjective robust optimization”, *Struct Multidiscip Optim*, 44(1), 99-110, 2011.

[13] Yin HF, Wen GL, Hou SJ, Chen K, “Crushing analysis and multiobjective crashworthiness optimization of honeycomb-filled single and bitubular polygonal tubes”, *Mater Des*, 32(8-9), 4449-4460, 2011.

[14] Guangyong Sun, Guangyao Li, Shiwei Zhou, Hongzhou Li, Shujuan Hou, Qing Li, “Crashworthiness design of vehicle by using multiobjective robust optimization”, *Structural and Multidisciplinary Optimization*, 44(1), 99-110, 2011.

[15] Craig KJ, Stander N, Dooge DA, Varadappa S, “Automotive crashworthiness design using response surface-based variable screening and optimization”, *Eng Comput*, 22(1-2), 38-61, 2005.

[16] Lei Shi, R. J. Yang, Ping Zhu, “A method for selecting surrogate models in crashworthiness optimization”, *Structural and Multidisciplinary Optimization*, 46(2), 159-170, 2012.

[17] Hu Wang, Enying Li, G. Y. Li., “Probability-based least square support vector regression metamodeling technique for crashworthiness optimization problems”, *Computational Mechanics*, 47(3), 251-263, 2011.

[18] Redhe M, Nilsson LA, “Multipoint version of space mapping optimization applied to vehicle crashworthiness design”, *Struct Multidiscip Opt*, 31(2), 134-146, 2006.